



IUCrData

ISSN 2414-3146

# Bepotastine besylate

Jacob K. Salazar,<sup>a</sup> James A. Kaduk,<sup>b,c,\*</sup> Anja Dosen<sup>d</sup> and Thomas N. Blanton<sup>e</sup>

<sup>a</sup>North Central College, Department of Chemistry, 131 S. Loomis St., Naperville, IL 60540, USA, <sup>b</sup>North Central College, Department of Physics, 131 S. Loomis St., Naperville, IL 60540, USA, <sup>c</sup>Illinois Institute of Technology, Department of Chemistry, 3101 S. Dearborn St., Chicago, IL 60616, USA, <sup>d</sup>ICDD, 12 Campus Blvd, Newtown Square, PA 19073-3273, USA, and <sup>e</sup>ICDD, 12 Campus Blvd., Newtown Square, PA 19073-3273, USA. \*Correspondence e-mail: kaduk@polycrystallography.com

Received 25 March 2026

Accepted 21 April 2026

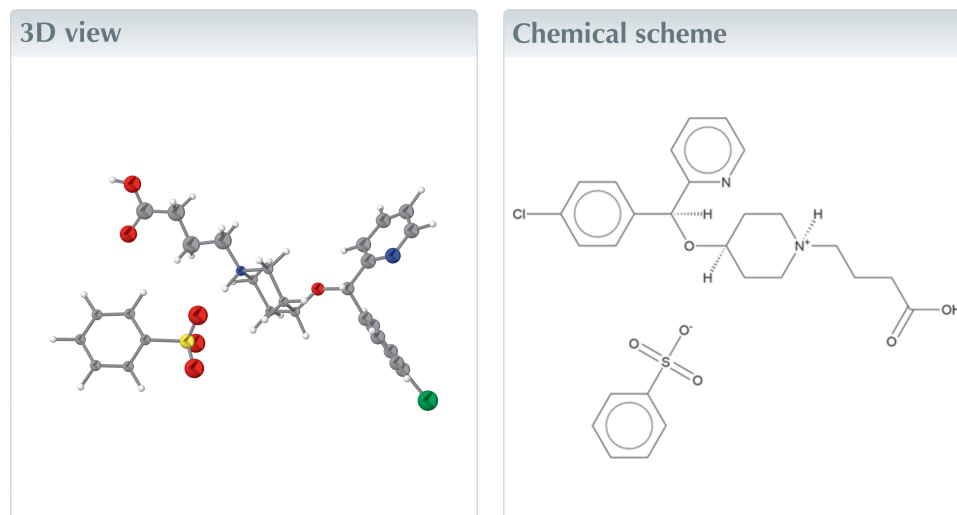
Edited by M. Zeller, Purdue University, USA

**Keywords:** powder diffraction; bepotastine; bepreve; Rietveld refinement; density functional theory; DFT.

CCDC reference: 2548211

**Structural data:** full structural data are available from iucrdata.iucr.org

The crystal structure of bepotastine besylate {systematic name: 1-(3-carboxypropyl)-4-[(4-chlorophenyl)(pyridin-2-yl)methoxy]piperidin-1-ium benzenesulfonate,  $C_{21}H_{26}ClN_2O_3^+ \cdot C_6H_5O_3S^-$ ) was refined using synchrotron X-ray powder diffraction data, and optimized using density functional theory techniques. Bepotastine besylate crystallizes in the space group  $P1$ , with  $a = 8.0153$  (6),  $b = 9.8211$  (5),  $c = 10.2345$  (10) Å,  $\alpha = 88.164$  (2),  $\beta = 68.962$  (2),  $\gamma = 65.8917$  (8)°,  $V = 680.149$  (1) Å<sup>3</sup> and  $Z = 1$  at 298 K. N—H...O and O—H...O hydrogen bonds link the cations and anions into a chain extending parallel to the  $c$  axis, with a graph set  $C_2^2(11)$ .



## Structure description

The r.m.s. Cartesian displacement between the recently-determined single-crystal (Wang *et al.*, 2025) and Rietveld-refined structures is 0.13 Å, the difference between the Rietveld-refined and *VASP*-optimized structures is 0.14 Å (*VASP* = Vienna Ab Initio Simulation Package; Kresse & Furthmüller, 1996). As expected, the model refined from single-crystal X-ray data and the model optimized with *VASP* are essentially identical. The Rietveld-refined model is almost as good. All of the differences are well within the normal range for correct structures (van de Streek & Neumann, 2014). The asymmetric unit with the atom numbering is presented in Fig. 1. The rest of this discussion will concentrate on the *VASP*-optimized structure.

All of the bond lengths, bond angles, and torsion angles fall within the normal ranges indicated by a *Mercury Mogul* Geometry check (Macrae *et al.*, 2020). Quantum chemical geometry optimization of the isolated cation (DFT/B3LYP/6-31G\*/water) using *Spartan '24* (Wavefunction, 2025) indicated that the solid-state conformation is 20.6 kJ mol<sup>-1</sup> higher in energy than a local minimum. The global minimum-energy conformation is

**Table 1**  
Hydrogen-bond geometry (Å, °).

$D-H\cdots A$	$D-H$	$H\cdots A$	$D\cdots A$	$D-H\cdots A$	Mulliken overlap	H-bond energy
O3–H3···O4	1.023	1.651	2.639	166.3		
N2–H2···O6	1.065	1.681	2.745	174.2		
<i>VASP</i> -optimized structure						
O3–H3···O4	1.023	1.651	2.639	166.3	0.067	14.0
N2–H2···O6	1.065	1.681	2.745	174.2	0.075	6.3
C2–H2A···O4	1.091	2.814	3.850	157.4	0.010	
C3–H3A···O6	1.098	2.581	3.341	127.8	0.012	
C4–H4···O1	1.101	2.471	2.786	95.1	0.010	
C6–H2···O2	1.107	2.491	3.570	170.8	0.013	
C8–H8···O4	1.102	2.881	3.903	161.0	0.010	
C9–H9···O2	1.092	2.489	3.517	158.7	0.019	
C11–H11···O5	1.100	2.188	3.176	152.8	0.034	
C13–H13A···Cl1	1.098	3.044	4.137	170.2	0.013	
C14–H14B···O5	1.099	2.568	3.461	139.4	0.014	
C15–H15···C7	1.100	2.681	3.045	99.2	0.014	
C16–H16A···O3	1.100	2.612	3.534	139.4	0.011	
C17–H17A···O1	1.098	2.675	2.972	93.9	0.010	

208.2 kJ mol<sup>-1</sup> lower in energy, but is much more compact (folded on itself). Intermolecular interactions are thus important to determining conformation in the solid-state.

The isotropic displacement coefficients from this Rietveld refinement tend to be smaller than the equivalent  $U_{\text{iso}}$  calculated from the anisotropic coefficients of the single-crystal refinement. The difference may indicate an imperfect absorption model in the Rietveld refinement. The  $\mu R$  was calculated using the tool on the 11-BM website (<https://11b.x-ray.aps.anl.gov/absorb/>), assuming a packing density of 50%. The packing density was not actually measured.

The availability of a structure refined from both single-crystal and powder data provides an opportunity to compare the precision (as well as the accuracy) of the two structures. The average standard uncertainties on the fractional coordinates are about three times larger in the structure refined from

powder data than in the single-crystal one. The powder structure is thus accurate, but less precise than the single-crystal result.

The crystal structure (Fig. 2) can be considered as layers parallel to the  $bc$  plane when viewed down the  $b$  axis, or as layers parallel to the  $(1\bar{1}0)$  plane when viewed down the  $c$  axis. The *Mercury* Aromatics Analyser indicates one strong interaction (4.87 Å) between the cation and anion. Other interactions are weak, with  $d > 8.02$  Å.

Analysis of the contributions to the total crystal energy of the structure using the Forcite module of *Materials Studio* (Dassault Systèmes, 2024) suggests that the intramolecular deformation energy is dominated by angle distortion terms, while van der Waals attractions (which in this force field-based analysis include hydrogen bonds) dominate the intermolecular energy.

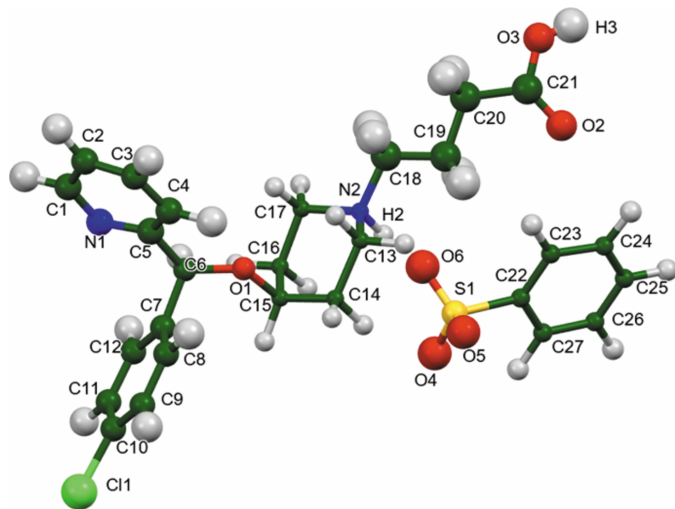


**Figure 1**  
The asymmetric unit of bepotastine besylate, with the atom numbering. The atoms are represented by 50% probability spheroids/ellipsoids. Image generated using *Mercury* (Macrae *et al.*, 2020).

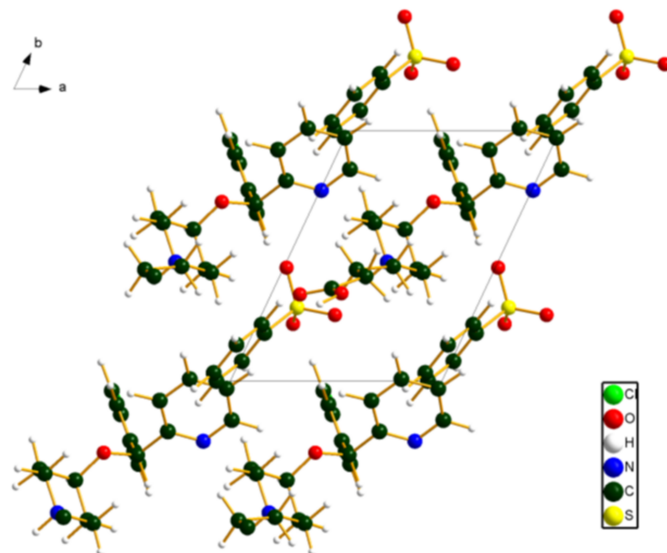


**Figure 2**  
The crystal structure of bepotastine besylate, viewed down the  $c$  axis. Image generated using *DIAMOND* (Crystal Impact, 2025).

There are two classical hydrogen bonds in the crystal structure (Table 1). The cation makes a O3—H3···O4 hydrogen bond to the anion, as well as an N2—H2···O6 one. These link the cations and anions into chains extending parallel to the *c* axis, with graph set (Etter, 1990; Bernstein *et al.*, 1995; Motherwell *et al.*, 2000)  $C_2^2(11)$ . The energy of the O—H···O hydrogen bond was calculated using the correlation of Rammohan & Kaduk (2018), and the energy of the N—H···O hydrogen bond was calculated using the correlation of Wheatley & Kaduk (2019). Several C—H···O/Cl/C hydrogen bonds also contribute to the lattice energy (Table 1).

The Bravais–Friedel–Donnay–Harker (Bravais, 1866; Friedel, 1907; Donnay & Harker, 1937) morphology suggests that we might expect isotropic morphology for bepotastine besylate. A second-order spherical harmonic model was included in the refinement. The texture index was 1.006 (0), indicating that preferred orientation was not significant in this rotated capillary specimen.

## Synthesis and crystallization

Bepotastine besylate was a white powder purchased from TargetMol (Batch No. 132062), and was used as received.

## Refinement

Crystal data, data collection, and structure refinement details are summarized in Table 2. Reflections were indexed using *JADE Pro* (MDI, 2025) and the crystal structure was solved independently using direct methods as implemented in *EXPO2014* (Altomare *et al.*, 2013). Before refinement, we discovered the Wang *et al.* (2025) publication of this structure

**Table 2**

Experimental details.

Crystal data	
Chemical formula	$C_{21}H_{26}ClN_2O_3^+ \cdot C_6H_5O_3S^-$
$M_r$	547.07
Crystal system, space group	Triclinic, $P1$
Temperature (K)	298
$a, b, c$ (Å)	8.0153 (6), 9.8211 (5), 10.2345 (10)
$\alpha, \beta, \gamma$ (°)	88.1641 (17), 68.962 (2), 65.8917 (8)
$V$ (Å <sup>3</sup> )	680.12 (2)
$Z$	1
Radiation type	Synchrotron, $\lambda = 0.81933$ Å
Specimen shape, size (mm)	Cylinder, 0.45 × 0.15
Data collection	
Diffractometer	Wiggler Low-Energy Beamline, Brockhouse X-ray Diffraction and Scattering Sector, Canadian Light Source
Specimen mounting	Kapton capillary
Data collection mode	Transmission
Scan method	Step
$2\theta$ values (°)	$2\theta_{\min} = -9.008$ $2\theta_{\max} = 75.047$ , $2\theta_{\text{step}} = 0.003$
Refinement	
$R$ factors and goodness of fit	$R_p = 0.018$ , $R_{wp} = 0.027$ , $R_{\text{exp}} = 0.002$ , $R(F^2) = 0.04412$ , $\chi^2 = 125.956$
No. of parameters	157
No. of restraints	94
$(\Delta/\sigma)_{\max}$	2.333

Computer program: *GSAS-II* (Toby & Von Dreele, 2013).

[it has not yet (as of March 2026) been added to the Cambridge Structural Database (Groom *et al.*, 2016)], and used their atom numbering.

Rietveld refinement (Fig. 3) was carried out using *GSAS-II* (Toby & Von Dreele, 2013). All non-hydrogen-bond lengths

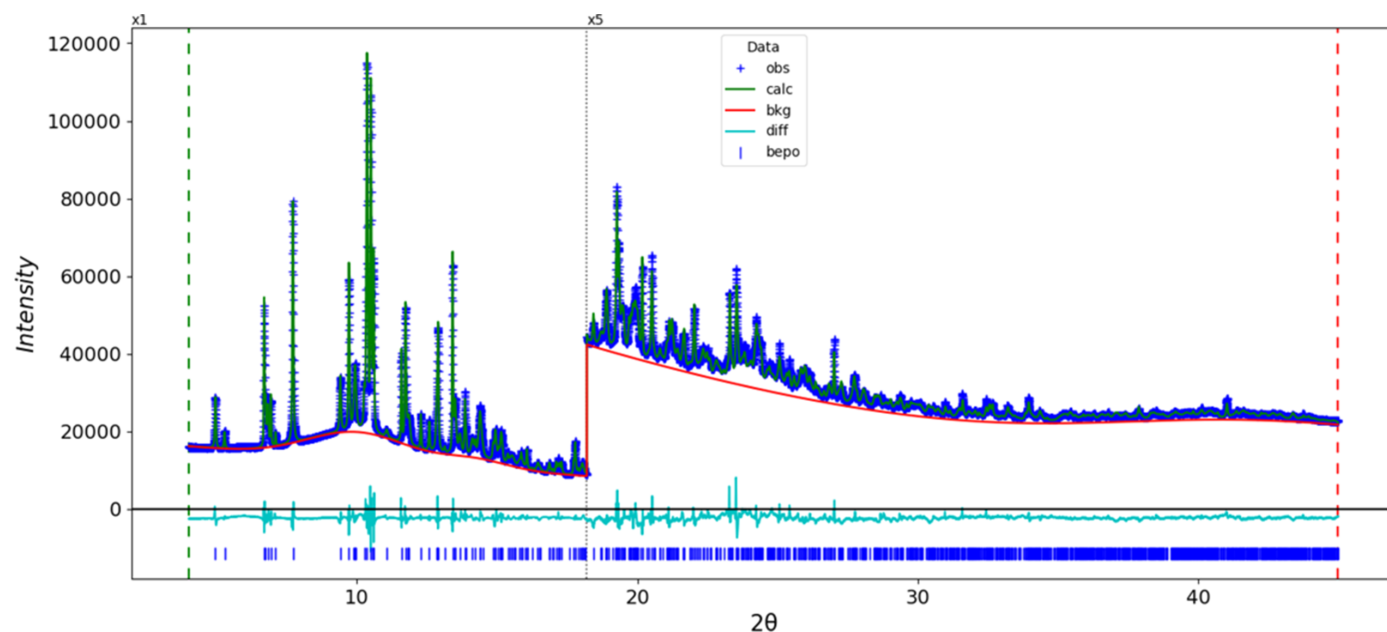


**Figure 3**

The Rietveld plot for bepotastine besylate. The blue crosses represent the observed data points, and the green line is the calculated pattern. The cyan curve is the normalized error plot, and the red line is the background curve. The blue tick marks indicate the peak positions. The vertical scale has been multiplied by a factor of  $\times 5$  for  $2\theta > 18.2^\circ$ .

and angles were restrained according to a *Mercury/Mogul* Geometry Check (Sykes *et al.*, 2011; Bruno *et al.*, 2004). H atoms were included in calculated positions and recalculated during the refinement using the Adjust Hydrogen tool of *Materials Studio* (Dassault Systèmes, 2024). The coordinates of atom Cl1 were fixed to define the origin.  $U_{\text{iso}}$  of the C, N, and O atoms were grouped by chemical similarity, while the  $U_{\text{iso}}$  for H atoms were fixed at 1.3 times the  $U_{\text{iso}}$  of the C, N, and O atoms to which they are attached. Attempts to refine the Cl atom anisotropically led to an unreasonable ellipsoid, so it was refined isotropically. The final refinement yielded  $R_{\text{wp}} = 0.02700$ . The largest features in the normalized error plot are in the shapes of many of the strong low-angle reflections. In the difference-Fourier map, the residual maximum (1.98 Å from O2) and minimum (1.76 Å from C2) electron-density peaks were 0.16 (4) and  $-0.20$  (4)  $\text{e} \text{ \AA}^{-3}$ , respectively.

The crystal structure of bepotastine besylate was optimized (fixed Rietveld-refined unit cell) with density functional theory techniques using *VASP* (Version 6.0; Kresse & Furthmüller, 1996) through the *MedeA* graphical interface (Materials Design, 2024). Single-point density functional theory calculations (fixed experimental cell) and population analysis were carried out with *CRYSTAL23* (Erba *et al.*, 2023) using H, C, N, and O basis sets defined by Gatti *et al.* (1994) and the basis sets for S and Cl of Peintinger *et al.* (2013).

The powder pattern has been submitted to ICDD (International Centre for Diffraction Data) for inclusion in the Powder Diffraction File (PDF). The structure has been determined simultaneously using single-crystal techniques (Wang *et al.*, 2025).

## Acknowledgements

Part of the research described in this paper was performed at the Canadian Light Source (Leontowich *et al.*, 2021), a national research facility of the University of Saskatchewan, which is supported by the Canada Foundation for Innovation (CFI), the Natural Sciences and Engineering Research Council (NSERC), the Canadian Institute of Health Research (CIHR), the Government of Saskatchewan, and the University of Saskatchewan. We thank Adam Leontowich for his assistance in the data collection. We also thank the ICDD team - Megan Rost, Steve Trimble, and Dave Bohnenberger – for their contribution to research, sample preparation, and in-house XRD data collection and verification.

## Funding information

Funding for this research was provided by: International Centre for Diffraction Data (grant No. 09-03).

## References

- Altomare, A., Cuocci, C., Giacobozzo, C., Moliterni, A., Rizzi, R., Corriero, N. & Falcicchio, A. (2013). *J. Appl. Cryst.* **46**, 1231–1235.
- Bernstein, J., Davis, R. E., Shimoni, L. & Chang, N. L. (1995). *Angew. Chem. Int. Ed. Engl.* **34**, 1555–1573.
- Bravais, A. (1866). *Etudes Cristallographiques*. Paris, Gauthier Villars.
- Bruno, I. J., Cole, J. C., Kessler, M., Luo, J., Motherwell, W. D. S., Purkis, L. H., Smith, B. R., Taylor, R., Cooper, R. I., Harris, S. E. & Orpen, A. G. (2004). *J. Chem. Inf. Comput. Sci.* **44**, 2133–2144.
- Crystal Impact (2025). *DIAMOND*. Version 5.1.1. Crystal Impact GbR, Bonn, Germany.
- Dassault Systèmes (2024). *BIOVIA Materials Studio 2025*. BIOVIA, San Diego, CA, USA.
- Donnay, J. D. H. & Harker, D. (1937). *Am. Mineral.* **22**, 446–467.
- Erba, A., Desmarais, J. K., Casassa, S., Civalleri, B., Donà, L., Bush, I. J., Searle, B., Maschio, L., Edith-Daga, L., Cossard, A., Ribaldone, C., Ascricchi, E., Marana, N. L., Flament, J.-P. & Kirtman, B. (2023). *J. Chem. Theory Comput.* **19**, 6891–6932.
- Etter, M. C. (1990). *Acc. Chem. Res.* **23**, 120–126.
- Friedel, G. (1907). *Bull. Soc. Française Minéral.* **30**, 326–455.
- Gatti, C., Saunders, V. R. & Roetti, C. (1994). *J. Chem. Phys.* **101**, 10686–10696.
- Groom, C. R., Bruno, I. J., Lightfoot, M. P. & Ward, S. C. (2016). *Acta Cryst. B* **72**, 171–179.
- Kresse, G. & Furthmüller, J. (1996). *Comput. Mater. Sci.* **6**, 15–50.
- Leontowich, A. F. G., Gomez, A., Diaz Moreno, B., Muir, D., Spasyuk, D., King, G., Reid, J. W., Kim, C.-Y. & Kycia, S. (2021). *J. Synchrotron Rad.* **28**, 961–969.
- Macrae, C. F., Sovago, I., Cottrell, S. J., Galek, P. T. A., McCabe, P., Pidcock, E., Platings, M., Shields, G. P., Stevens, J. S., Towler, M. & Wood, P. A. (2020). *J. Appl. Cryst.* **53**, 226–235.
- Materials Design (2024). *MedeA*. Version 3.7.2. Materials Design Inc., San Diego, USA.
- MDI (2025). *JADE Pro*. Version 9.3. Materials Data, Livermore, USA.
- Motherwell, W. D. S., Shields, G. P. & Allen, F. H. (2000). *Acta Cryst. B* **56**, 857–871.
- Peintinger, M. F., Oliveira, D. V. & Bredow, T. (2013). *J. Comput. Chem.* **34**, 451–459.
- Rammohan, A. & Kaduk, J. A. (2018). *Acta Cryst. B* **74**, 239–252.
- Streek, J. van de & Neumann, M. A. (2014). *Acta Cryst. B* **70**, 1020–1032.
- Sykes, R. A., McCabe, P., Allen, F. H., Battle, G. M., Bruno, I. J. & Wood, P. A. (2011). *J. Appl. Cryst.* **44**, 882–886.
- Toby, B. H. & Von Dreele, R. B. (2013). *J. Appl. Cryst.* **46**, 544–549.
- Wang, F., Luan, L., Hu, X., Zhang, C. & Liu, Y. (2025). *Z. Kristallogr. New Cryst. Struct.* **240**, 579–580.
- Wavefunction, Inc. (2025). *Spartan '24*. Wavefunction Inc., Irvine, USA.
- Wheatley, A. M. & Kaduk, J. A. (2019). *Powder Diffr.* **34**, 35–43.

## full crystallographic data

*IUCrData* (2026). **11**, x260424 [https://doi.org/10.1107/S2414314626004244]

## Bepostastine besylate

Jacob K. Salazar, James A. Kaduk, Anja Dosen and Thomas N. Blanton

## 1-(3-Carboxypropyl)-4-[(4-chlorophenyl)(pyridin-2-yl)methoxy]piperidin-1-ium benzenesulfonate

## Crystal data

$C_{21}H_{26}ClN_2O_3^+ \cdot C_6H_5O_3S^-$

$M_r = 547.07$

Triclinic, *P*1

$a = 8.0153$  (6) Å

$b = 9.8211$  (5) Å

$c = 10.2345$  (10) Å

$\alpha = 88.1641$  (17)°

$\beta = 68.962$  (2)°

$\gamma = 65.8917$  (8)°

$V = 680.12$  (2) Å<sup>3</sup>

$Z = 1$

$D_x = 1.336$  Mg m<sup>-3</sup>

Synchrotron radiation,  $\lambda = 0.81933$  Å

$T = 298$  K

cylinder, 0.45 × 0.15 mm

## Data collection

Wiggler Low-Energy Beamline, Brockhouse X-ray Diffraction and Scattering Sector, Canadian Light Source diffractometer

Specimen mounting: Kapton capillary

Data collection mode: transmission

Scan method: step

$2\theta_{\min} = -9.008^\circ$ ,  $2\theta_{\max} = 75.047^\circ$ ,  $2\theta_{\text{step}} = 0.003^\circ$

## Refinement

Least-squares matrix: full

$R_p = 0.018$

$R_{\text{wp}} = 0.027$

$R_{\text{exp}} = 0.002$

$R(F^2) = 0.04412$

33623 data points

Profile function: Finger-Cox-Jephcoat function

parameters  $U$ ,  $V$ ,  $W$ ,  $X$ ,  $Y$ ,  $SH/L$ : peak

variance(Gauss) =  $U \tan(\text{Th})^2 + V \tan(\text{Th}) + W$ :

peak HW(Lorentz) =  $X / \cos(\text{Th}) + Y \tan(\text{Th})$ ;

$SH/L = S/L + H/L$   $U$ ,  $V$ ,  $W$  in (centideg)<sup>2</sup>,  $X$  &  $Y$

in centideg 6.157, -1.198, 1.258, 0.000, 0.667,

0.002,

157 parameters

94 restraints

28 constraints

Weighting scheme based on measured s.u.'s

$(\Delta/\sigma)_{\max} = 2.333$

Background function: Background function:

"chebyshev-1" function with 3 terms:

7.82(4)e3, -6.61(6)e3, 1.72(3)e3, Background

peak parameters: pos, int, sig, gam: 10.042(8),

3.336(18)e6, 3.30(4)e4, 0.100, 14.208(20),

7.15(14)e5, 1.43(4)e4, 0.100, 41.97(20),

2.36(23)e6, 3.42(23)e5, 0.100,

Preferred orientation correction: Simple

spherical harmonic correction Order = 2

Coefficients: 0:0:C(2,-2) = 0.042(5); 0:0:C(2,-1)

= 0.110(6); 0:0:C(2,0) = 0.009(7); 0:0:C(2,1) =

-0.134(5); 0:0:C(2,2) = 0.031(5)

Fractional atomic coordinates and isotropic or equivalent isotropic displacement parameters (Å<sup>2</sup>)

	<i>x</i>	<i>y</i>	<i>z</i>	$U_{\text{iso}}^*/U_{\text{eq}}$
Cl1	0.50540	0.93250	-0.60523	0.082 (3)*
O1	0.5505 (16)	0.7147 (12)	0.0188 (10)	0.034 (4)*
O2	0.116 (2)	0.3636 (16)	0.7826 (12)	0.059 (3)*
O3	0.3338 (16)	0.3491 (14)	0.8727 (12)	0.059 (3)*

---

H3	0.29300	0.30400	0.94400	0.0778*
N1	0.9969 (14)	0.7676 (10)	-0.1821 (9)	0.046 (3)*
N2	0.4631 (16)	0.4856 (11)	0.2721 (11)	0.020 (3)*
H2	0.40680	0.40890	0.25650	0.0255*
C1	1.0962 (17)	0.8438 (16)	-0.1643 (13)	0.046 (3)*
H1	1.25014	0.81896	-0.24501	0.0595*
C2	1.0220 (19)	0.9541 (17)	-0.0509 (15)	0.046 (3)*
H2A	1.11912	1.00663	-0.03757	0.0595*
C3	0.832 (2)	0.9940 (16)	0.0402 (12)	0.046 (3)*
H3A	0.75694	1.09371	0.12692	0.0595*
C4	0.7301 (16)	0.9122 (16)	0.0268 (13)	0.046 (3)*
H4	0.57426	0.94103	0.10643	0.0595*
C5	0.8204 (13)	0.7980 (13)	-0.0828 (12)	0.046 (3)*
C6	0.7188 (15)	0.7061 (11)	-0.1060 (9)	0.034 (4)*
H6	0.83146	0.58331	-0.13717	0.0444*
C7	0.6533 (17)	0.7563 (11)	-0.2276 (9)	0.041 (3)*
C8	0.510 (2)	0.8993 (12)	-0.2153 (9)	0.041 (3)*
H8	0.43155	0.97627	-0.11032	0.0624*
C9	0.4590 (19)	0.9524 (10)	-0.3287 (10)	0.041 (3)*
H9	0.33604	1.06955	-0.31503	0.0624*
C10	0.559 (2)	0.8612 (11)	-0.4575 (8)	0.041 (3)*
C11	0.7068 (18)	0.7186 (10)	-0.4722 (9)	0.041 (3)*
H11	0.78915	0.64441	-0.57890	0.0534*
C12	0.7522 (18)	0.6682 (10)	-0.3570 (10)	0.041 (3)*
H12	0.87456	0.55082	-0.37036	0.0534*
C13	0.3185 (17)	0.6382 (13)	0.2781 (11)	0.020 (3)*
H13A	0.37653	0.72188	0.29482	0.0255*
H13B	0.17356	0.66131	0.37000	0.0255*
C14	0.2792 (16)	0.6589 (15)	0.1392 (14)	0.020 (3)*
H14A	0.17877	0.78213	0.14286	0.0253*
H14B	0.20237	0.58660	0.12936	0.0255*
C15	0.4635 (18)	0.6143 (15)	0.0121 (11)	0.020 (3)*
H15	0.43091	0.62040	-0.08812	0.0255*
C16	0.6116 (17)	0.4627 (13)	0.0115 (12)	0.020 (3)*
H16A	0.55409	0.37582	0.00356	0.0255*
H16B	0.75479	0.43672	-0.08318	0.0255*
C17	0.6513 (15)	0.4550 (13)	0.1465 (13)	0.020 (3)*
H17A	0.70654	0.54294	0.15589	0.0255*
H17B	0.76819	0.33815	0.14360	0.0255*
C18	0.495 (2)	0.4649 (17)	0.4089 (13)	0.059 (3)*
H18A	0.49294	0.57254	0.44961	0.0773*
H18B	0.64553	0.36826	0.38954	0.0773*
C19	0.349 (2)	0.430 (2)	0.5176 (14)	0.059 (3)*
H19A	0.35115	0.32131	0.47972	0.0773*
H19B	0.19654	0.52637	0.54307	0.0773*
C20	0.404 (2)	0.410 (2)	0.6477 (14)	0.059 (3)*
H20A	0.54754	0.30528	0.62425	0.0773*
H20B	0.42765	0.51206	0.67129	0.0773*

C21	0.2547 (19)	0.3924 (17)	0.7812 (13)	0.059 (3)*
S1	0.1428 (11)	0.3047 (8)	0.2397 (8)	0.043 (3)*
O4	0.1779 (16)	0.2340 (12)	0.1101 (12)	0.072 (3)*
O5	-0.0095 (17)	0.4590 (12)	0.2794 (12)	0.072 (3)*
O6	0.3278 (18)	0.2767 (14)	0.2400 (13)	0.072 (3)*
C22	0.053 (2)	0.1955 (14)	0.3627 (9)	0.023 (3)*
C23	0.028 (2)	0.2166 (15)	0.5031 (11)	0.023 (3)*
H23	0.07729	0.29738	0.53849	0.0299*
C24	-0.059 (2)	0.1374 (15)	0.5982 (10)	0.023 (3)*
H24	-0.09068	0.15850	0.71538	0.0299*
C25	-0.106 (2)	0.0357 (16)	0.5530 (12)	0.023 (3)*
H25	-0.16802	-0.03343	0.63058	0.0299*
C26	-0.079 (3)	0.0132 (16)	0.4144 (14)	0.023 (3)*
H26	-0.12166	-0.07253	0.37851	0.0299*
C27	-0.002 (2)	0.0933 (16)	0.3172 (11)	0.023 (3)*
H27	0.01667	0.07747	0.20196	0.0299*

*Geometric parameters (Å, °)*

C11—C10	1.765 (6)	H14A—C14	1.140 (12)
O1—C6	1.461 (8)	H14B—C14	1.140 (12)
O1—C15	1.437 (5)	C15—O1	1.437 (5)
O2—C21	1.247 (8)	C15—C14	1.481 (8)
O3—H3	0.873 (9)	C15—H15	1.141 (9)
O3—C21	1.281 (9)	C15—C16	1.476 (8)
H3—O3	0.873 (9)	H15—C15	1.141 (9)
N1—C1	1.352 (6)	C16—C15	1.476 (8)
N1—C5	1.329 (5)	C16—H16A	1.140 (11)
N2—H2	1.065 (9)	C16—H16B	1.140 (10)
N2—C13	1.460 (7)	C16—C17	1.518 (8)
N2—C17	1.510 (7)	H16A—C16	1.140 (11)
N2—C18	1.504 (8)	H16B—C16	1.140 (10)
H2—N2	1.065 (9)	C17—N2	1.510 (7)
C1—N1	1.352 (6)	C17—C16	1.518 (8)
C1—H1	1.140 (9)	C17—H17A	1.140 (12)
C1—C2	1.391 (8)	C17—H17B	1.140 (10)
H1—C1	1.140 (9)	H17A—C17	1.140 (12)
C2—C1	1.391 (8)	H17B—C17	1.140 (10)
C2—H2A	1.140 (10)	C18—N2	1.504 (8)
C2—C3	1.363 (7)	C18—H18A	1.140 (14)
H2A—C2	1.140 (10)	C18—H18B	1.140 (14)
C3—C2	1.363 (7)	C18—C19	1.446 (10)
C3—H3A	1.140 (8)	H18A—C18	1.140 (14)
C3—C4	1.399 (6)	H18B—C18	1.140 (14)
H3A—C3	1.140 (8)	C19—C18	1.446 (10)
C4—C3	1.399 (6)	C19—H19A	1.140 (18)
C4—H4	1.140 (8)	C19—H19B	1.140 (19)
C4—C5	1.369 (6)	C19—C20	1.527 (10)

H4—C4	1.140 (8)	H19A—C19	1.140 (18)
C5—N1	1.329 (5)	H19B—C19	1.140 (19)
C5—C4	1.369 (6)	C20—C19	1.527 (10)
C5—C6	1.512 (4)	C20—H20A	1.140 (18)
C6—O1	1.461 (8)	C20—H20B	1.140 (17)
C6—C5	1.512 (4)	C20—C21	1.519 (7)
C6—H6	1.140 (10)	H20A—C20	1.140 (18)
C6—C7	1.512 (5)	H20B—C20	1.140 (17)
H6—C6	1.140 (10)	C21—O2	1.247 (8)
C7—C6	1.512 (5)	C21—O3	1.281 (9)
C7—C8	1.377 (5)	C21—C20	1.519 (7)
C7—C12	1.375 (5)	S1—O4	1.397 (9)
C8—C7	1.377 (5)	S1—O5	1.458 (8)
C8—H8	1.139 (8)	S1—O6	1.394 (9)
C8—C9	1.384 (6)	S1—C22	1.774 (5)
H8—C8	1.139 (8)	O4—S1	1.397 (9)
C9—C8	1.384 (6)	O5—S1	1.458 (8)
C9—H9	1.140 (8)	O6—S1	1.394 (9)
C9—C10	1.383 (6)	C22—S1	1.774 (5)
H9—C9	1.140 (8)	C22—C23	1.388 (5)
C10—C11	1.765 (6)	C22—C27	1.401 (5)
C10—C9	1.383 (6)	C23—C22	1.388 (5)
C10—C11	1.384 (6)	C23—H23	1.140 (9)
C11—C10	1.384 (6)	C23—C24	1.392 (6)
C11—H11	1.140 (8)	H23—C23	1.140 (9)
C11—C12	1.375 (5)	C24—C23	1.392 (6)
H11—C11	1.140 (8)	C24—H24	1.140 (10)
C12—C7	1.375 (5)	C24—C25	1.346 (7)
C12—C11	1.375 (5)	H24—C24	1.140 (10)
C12—H12	1.140 (7)	C25—C24	1.346 (7)
H12—C12	1.140 (7)	C25—H25	1.140 (9)
C13—N2	1.460 (7)	C25—C26	1.369 (8)
C13—H13A	1.140 (12)	H25—C25	1.140 (9)
C13—H13B	1.140 (11)	C26—C25	1.369 (8)
C13—C14	1.552 (8)	C26—H26	1.140 (10)
H13A—C13	1.140 (12)	C26—C27	1.377 (6)
H13B—C13	1.140 (11)	H26—C26	1.140 (10)
C14—C13	1.552 (8)	C27—C22	1.401 (5)
C14—H14A	1.140 (12)	C27—C26	1.377 (6)
C14—H14B	1.140 (12)	C27—H27	1.141 (9)
C14—C15	1.481 (8)	H27—C27	1.141 (9)
C6—O1—C15	117.3 (7)	C14—C15—H15	110.6 (9)
H3—O3—C21	124.8 (10)	O1—C15—C16	105.4 (6)
C1—N1—C5	117.5 (3)	C14—C15—C16	111.7 (5)
H2—N2—C13	108.3 (9)	H15—C15—C16	110.6 (10)
H2—N2—C17	108.2 (8)	C15—C16—H16A	109.4 (10)
C13—N2—C17	108.7 (5)	C15—C16—H16B	109.3 (10)

H2—N2—C18	108.3 (7)	H16A—C16—H16B	109.3 (8)
C13—N2—C18	110.6 (7)	C15—C16—C17	110.2 (4)
C17—N2—C18	112.6 (6)	H16A—C16—C17	109.1 (10)
N1—C1—H1	120.0 (8)	H16B—C16—C17	109.4 (10)
N1—C1—C2	123.8 (4)	N2—C17—C16	109.6 (5)
H1—C1—C2	116.2 (9)	N2—C17—H17A	109.5 (9)
C1—C2—H2A	120.0 (9)	C16—C17—H17A	109.4 (8)
C1—C2—C3	116.9 (5)	N2—C17—H17B	109.5 (9)
H2A—C2—C3	123.1 (10)	C16—C17—H17B	109.4 (10)
C2—C3—H3A	120.0 (10)	H17A—C17—H17B	109.5 (8)
C2—C3—C4	119.7 (4)	N2—C18—H18A	108.7 (10)
H3A—C3—C4	120.3 (9)	N2—C18—H18B	109.5 (9)
C3—C4—H4	120.0 (8)	H18A—C18—H18B	108.7 (10)
C3—C4—C5	119.0 (3)	N2—C18—C19	113.9 (7)
H4—C4—C5	121.0 (8)	H18A—C18—C19	108.7 (14)
N1—C5—C4	122.5 (3)	H18B—C18—C19	107.3 (12)
N1—C5—C6	115.2 (4)	C18—C19—H19A	109.8 (14)
C4—C5—C6	122.2 (4)	C18—C19—H19B	109.5 (14)
O1—C6—C5	113.8 (5)	H19A—C19—H19B	109.8 (10)
O1—C6—H6	108.0 (7)	C18—C19—C20	107.5 (6)
C5—C6—H6	108.0 (7)	H19A—C19—C20	109.8 (15)
O1—C6—C7	109.9 (6)	H19B—C19—C20	110.5 (15)
C5—C6—C7	109.1 (5)	C19—C20—H20A	109.5 (16)
H6—C6—C7	107.9 (5)	C19—C20—H20B	108.3 (13)
C6—C7—C8	120.0 (4)	H20A—C20—H20B	108.3 (10)
C6—C7—C12	120.6 (4)	C19—C20—C21	116.2 (6)
C8—C7—C12	118.9 (3)	H20A—C20—C21	106.0 (11)
C7—C8—H8	120.0 (6)	H20B—C20—C21	108.3 (12)
C7—C8—C9	121.1 (3)	O2—C21—O3	121.3 (8)
H8—C8—C9	118.9 (6)	O2—C21—C20	123.6 (8)
C8—C9—H9	120.0 (6)	O3—C21—C20	109.4 (8)
C8—C9—C10	118.9 (3)	O4—S1—O5	115.2 (7)
H9—C9—C10	121.1 (6)	O4—S1—O6	106.2 (7)
C11—C10—C9	119.2 (4)	O5—S1—O6	118.2 (7)
C11—C10—C11	120.3 (4)	O4—S1—C22	103.0 (4)
C9—C10—C11	120.5 (3)	O5—S1—C22	107.0 (5)
C10—C11—H11	120.0 (5)	O6—S1—C22	106.0 (5)
C10—C11—C12	119.3 (3)	S1—C22—C23	120.7 (4)
H11—C11—C12	120.8 (6)	S1—C22—C27	118.7 (4)
C7—C12—C11	121.3 (3)	C23—C22—C27	120.5 (3)
C7—C12—H12	120.0 (6)	C22—C23—H23	119.9 (7)
C11—C12—H12	118.7 (6)	C22—C23—C24	118.7 (3)
N2—C13—H13A	109.2 (9)	H23—C23—C24	121.4 (7)
N2—C13—H13B	109.4 (9)	C23—C24—H24	120.0 (8)
H13A—C13—H13B	109.2 (9)	C23—C24—C25	120.5 (4)
N2—C13—C14	110.9 (5)	H24—C24—C25	119.4 (8)
H13A—C13—C14	109.3 (10)	C24—C25—H25	120.0 (9)
H13B—C13—C14	108.7 (9)	C24—C25—C26	121.1 (4)

---

C13—C14—H14A	109.0 (11)	H25—C25—C26	118.9 (9)
C13—C14—H14B	109.5 (10)	C25—C26—H26	120.0 (9)
H14A—C14—H14B	108.9 (8)	C25—C26—C27	120.6 (4)
C13—C14—C15	112.5 (4)	H26—C26—C27	119.4 (8)
H14A—C14—C15	109.0 (9)	C22—C27—C26	118.5 (3)
H14B—C14—C15	108.0 (10)	C22—C27—H27	120.3 (7)
O1—C15—C14	107.7 (6)	C26—C27—H27	121.2 (7)
O1—C15—H15	110.6 (9)		

---

*Hydrogen-bond geometry (Å, °)*

---

<i>D</i> —H $\cdots$ <i>A</i>	<i>D</i> —H	H $\cdots$ <i>A</i>	<i>D</i> $\cdots$ <i>A</i>	<i>D</i> —H $\cdots$ <i>A</i>
O3—H3 $\cdots$ O4	1.023	1.651	2.639	166.3
N2—H2 $\cdots$ O6	1.065	1.681	2.745	174.2

---